# Global pattern of plasma bubbles irregularities at midnight using ion drift spectrometer measurements

**Article** *in* International Journal of Civil Engineering and Technology · October 2018

CITATIONS
0

READS
60

**5 authors**, including:

Babatunde Olufemi Adebesin
Landmark University
**54** PUBLICATIONS **230** CITATIONS
SEE PROFILE

Stephen O. IKUBANNI
Landmark University
**25** PUBLICATIONS **104** CITATIONS
SEE PROFILE

Shola J Adebiyi
Landmark University
**32** PUBLICATIONS **111** CITATIONS
SEE PROFILE

Dopamu Kehinde Oladele
Landmark University
**8** PUBLICATIONS **1** CITATION
SEE PROFILE

**xInternational Journal of Civil Engineering and Technology (IJCIET)**
Volume 9, Issue 10, October 2018, pp. 929–940, Article ID: IJCIET_09_10_094
Available online at http://www.iaeme.com/ijciet/issues.asp?JType=IJCIET&VType=9&IType=10
ISSN Print: 0976-6308 and ISSN Online: 0976-6316



# ARTICLE TITLE: GLOBAL PATTERN OF PLASMA BUBBLES IRREGULARITIES AT MIDNIGHT USING ION DRIFT SPECTROMETER MEASUREMENTS

***B. O. Adebesin, S. O. Ikubanni, S. J. Adebiyi and K. O. Dopamu**
Department of Physical Sciences, Space Weather Group,
Landmark University, Omu-Aran, Nigeria

**B. J. Adekoya**
Department of Physics, Olabisi Onabanjo University, Ago-Iwoye, Ogun State, Nigeria
*Corresponding Author

## ABSTRACT

*One of the anomalies which continue to receive much attention is the large-scale plasma depletions, the ionospheric plasma bubbles. Equatorial plasma bubble irregularity if not well monitored, can impair radio and Global Positioning System (GPS) navigations asides other systems. Consequently, the midnight seasonal and longitudinal variability of plasma bubbles occurrence rate had been presented. Data used spans January 1978-December 1979 (F10.7 = 143), and is obtained using the Atmospheric Explorer satellite ion drift meter. 18 longitudinal locations were examined and were divided into five sectors (African, Indian, Pacific, American and Atlantic) across the globe. The percentage occurrence rates ($\%_R$) of the bubbles revealed 10, 39, 34, and 16% for March and September equinoxes, June solstice, and December solstices respectively, with the highest activity in the African-Atlantic sector for all seasons. Seasons with the highest $\%_R$ are characterized with corresponding higher correlation coefficients (R) of total number of trips ($T_T$) to trips with bubbles ($T_B$) relation. June solstice and September equinox recorded higher $T_T/T_B$ correlation relation values of R = 0.8270 and 0.7543 respectively. The occurrence activity rate of $D_B$ , the percentage ratio of number of bubbles (B) relative to the number of trips with bubbles ($T_B$) is lower during the solstices when compared with equinoxes for all longitudinal sectors. We suggested that the correlation value for the $T_T/T_B$ relation is an indicator of the occurrence rate magnitude both seasonally and longitudinally. Past results especially in the Pacific sector were also confirmed.*

**Keywords**: ionosphere; solstice; equatorial plasma bubbles; GPS navigation; equator; electrodynamics.

**Cite this Article:** B. O. Adebesin, S. O. Ikubanni, S. J. Adebiyi, B. J. Adekoya and K. O. Dopamu, Article Title: Global Pattern of Plasma Bubbles Irregularities at Midnight using Ion Drift Spectrometer Measurements, International Journal of Civil Engineering and Technology, 9(10), 2018, pp. 929–940.

http://www.iaeme.com/IJCIET/issues.asp?JType=IJCIET&VType=9&IType=10

# 1. INTRODUCTION

Equatorial nighttime ionospheric abnormalities in the upper ionospheric layer have been the focus of space weather investigations of late (e.g. Adebesin et al., 2013a; Adebesin et al., 2014; Adebesin et al., 2015a). One of the anomalies which continue to receive much attention is the large-scale plasma depletions, the ionospheric plasma bubbles (Sahai et al., 1994; Adebiyi et al., 2014a). According to Burke et al (2004, and the reference therein), these anomalies/irregularities originally form at the bottom-side of the F-region ionosphere through the Rayleigh-Taylor (R-T) instability mechanism in connection with the E x B drift instability (Lee et al, 2005). Adebesin et al (2013a) had attributed the lifting of this bottom-side of the F-region ionosphere (which is directly related to the occurrence rate of plasma bubble) after local sunset, to two major effects – First is the recombination of molecular ions in the lower ionospheric region; and secondly, to the electrodynamical lifting of the upper ionosphere. Oyekola (2009) and Adebesin et al. (2015b) had attributed the equatorial ionospheric region post-sunset event as an important parameter controlling the generation/inhibition of the plasma instability at the ionospheric bottom-side region. The appearance of plasma bubbles in altitude-time ionograms and radar displays sometimes makes it to be referred to as range spread F (e.g. Aarons, 1993) or plasma plumes (e.g. Woodman and La Hoz, 1976) respectively. However, the frequency of occurrence of plasma bubble is characterized by strong seasonal-longitudinal variability (Huang et al., 2001; Aarons, 1993).

The investigation of the temporal reliabilities of the uneven equilibrium by Basu (1997) as evening period plasma flux tubes responds to variations in height level of the several force fields, is a good platform to explain plasma bubble generation. Two sources are attributed to the dusk sector eastward electric fields. First is as highlighted by Eccles (1998) and Adebesin et al, (2013b) in which case the solar quiet current leaks into the nighttside ionospheric layer. Second is the high latitude electric field diffusion into the low latitude (e.g. Burke et al., 2004; Adeniyi et al., 2014; Adebesin et al., 2016). This diffusion usually coincides with periods of enhanced polar cap potential just before the development of shielding, while the solar quiet is systemic (e.g. Burke et al., 1998). According to Adebesin et al (2013c, 2015a), the systemic vertical E x B drift are characterized by pre-reversal enhancements (PRE) immediately after sunset. However, in the early pre-sunset local time period, the negative polarization charge which originates near the terminator and subsequently develops causes initial plasma enhancement, and later reverses (around 2100h) in other for the F-layer bottom-side to be stabilize against irregularity formation. In-between this process, plasma bubbles can develop before damping forces set in. Consequently, three major elements which controls plasma bubbles generation can be highlighted as (i) evening time enhancement of the F-layer heights caused by atmospheric tides/plasma drifts, (ii) seeding mechanism of gravity waves, and (iii) large scale wave structure. Condition (ii) have been adjudged to be as a consequence of solar heating, and (the tides) are the major drive for the night-time and day-to-day plasma variability experienced in the ionosphere (Terra et al., 2004, Adebiyi et al., 2014b). It has been observed that bubbles occurrence increases with increase in solar activity,

and the bubbles are more frequent in specific seasons owning to longitudinal differences of stations (Gentile et al., 2006).

Consequently, a broad list of data for the longitudinal seasonal variation of plasma bubbles is necessary. A comprehensive assessment of the different observational procedures, as well as existing databases is found in the review work of Abdu (2001, and references therein). Investigating the characteristics and variability of plasma bubbles is of scientific interest as they can cause arbitrary fluctuations/errors and scintillations to ionospheric probing (in satellite signals) which can affect the effective functionality of communication and navigation systems on Earth (Adebiyi et al., 2014a; Adebesin et al. 2018a; Adebesin et al. 2018b). Figure 1 is a pictorial view of the impediments to communication system which may result from the action of plasma bubbles.

The aim of this work therefore is to examine the seasonal and longitudinal observations of midnight variability of plasma bubble occurrence from one sector of the world to another. It is worth mentioning that the study of plasma bubbles in the African sector had been understudied. In fact, the first ground-based plasma bubble/scintillation measuring equipment (the All Sky OI 630 nm optical airglow imager) in Africa was installed between June 7-10, 2015 in Abuja, Nigeria, (source: National Space Research and Development Agency, NASRDA, Abuja, Nigeria). It is believed that the results obtained from this work will go a long way in revealing the pattern of plasma bubble in the African sector, relative to other sectors of the world.

## 2. MATERIALS AND METHODS

The data used for this study spans two years, January 1978-December 1979, indicating moderate solar activity (F10.7 = 143) period. It was obtained by observations of the ion drift spectrometer on the Atmosphere Explorer Satellite which passes through the ionosphere. The Thor/Delta 2910 launch vehicle from the Eastern Test Range was used to launch the AE-E satellite on November 20, 1975, with the aim of providing measurements for studying the composition and processes within the thermosphere by probing into the atmosphere (see www.utd500.utdalass.edu/AE_data.html). The measurement is achieved by attaching high resolution and sensitive camera to the satellite and thereby obtaining two-dimensional images of the low-intensity light (often called airglow) which are weak and barely visible to natural eye, emanating from the upper part of the Earth's atmosphere. With this method, various patterns arising from plasma bubbles and gravity waves in the ionosphere are measured. The raw data obtained were modified using a three point running mean in other to get rid of any spurious fluctuations that might exist in the results. The data analysis is as follows. The percentage total numbers of satellite passes (trips) during midnight (0000h) were taken, whether or not they contain bubbles and denoted as $T_T$, then, a count of the percentage number of trips with bubbles as $T_B$, and finally a count of midnight count of the percentage total number of bubbles as $B$ in all the 16 longitudinal positions under consideration.

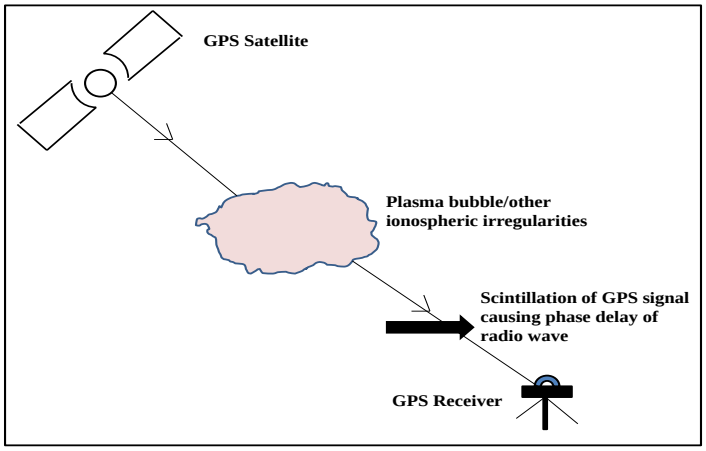


**Figure 1** Arbitrary fluctuations to communication/navigation systems on Earth as a consequence of the action of plasma bubble

From the readings obtained, the years were divided into four seasons, namely: March equinox (February-April), September equinox (August-October), June solstice (May-July), and December solstice (November-January) (e.g Adebesin et al., 2018c). From the above classes, the percentage mean number of bubbles per trip containing bubbles ($D_B$) was determined. $D_B$ is defined as the percentage ratio of overall number of bubbles ($B$) to the overall number of trips with bubbles ($T_B$). Similarly, the percentage mean number of bubbles per trip for all trips, $D_T$ , which is the $B/T_T$ ratio, is also determined. The entire 18 longitudinal locations were in the interval of 20 degrees ($0^0$, $20^0$, $40^0$, etc) and for descriptive convenience, are classified into five global sectors. The classification follows Burke et al. (2004) grouping, and are highlighted in Table 1.

**Table 1** Sectorial classifications of different longitudes

| Sector | Longitudinal range | |
|---|---|---|
| African | 00 - +450 | |
| Indian | +450 - +1100 | |
| Pacific | +1100 - +2400 | (or +1100 - -1200) |
| American | +2400 - +3100 | (or -1200 - -500) |
| Atlantic | +3100 - +3600 | (or -500 - 00) |

## 2. RESULTS

Figure 2 highlights the percentage seasonal plot of plasma bubble as a function of geographic longitude for the five global sectors under investigation. The vertical dashed lines across the entire plot demarcate the sectors accordingly. The figure shows different seasonal and longitudinal morphology between the five sectors. The highest rates of plasma bubble occurrence were recorded in the African-Atlantic sector for all seasons, whereas, the lowest detection rate was in the Indian sector during the equinoxes, at American sector during June solstice, and at Pacific sector during December solstice. The sectorial differences would have been caused by the strength of the geomagnetic field as well as the ionospheric F-layer. This is because most of the longitudinal locations considered have different magnetic declination angle, which is one of the parameters that controls plasma bubble occurrence (Nishioka et al, 2006, Adebesin et al, 2013a). The highest occurrence rate observation in the African-Atlantic sector is in consonance with Burke et al (2004) result. Burke et al (2004) had used data obtained from around 80,000 equatorial evening-sector passes of polar-orbiting DMSP satellites into 24 longitudes. Seasonally, we recorded the highest bubble occurrence rate

during September equinox, and in agreement with the submission of Maruyama and Matuura (1984). The least occurrence activity was in March equinox. The percentage occurrence rates of the bubbles are 10, 39, 34, and 16% for March and September equinoxes, June solstice, and December solstices respectively.

The bar chart of the variability in longitude and season of the percentage mean number of bubbles per trip containing bubbles ($D_B$) is shown in figure 3. The variation in $D_B$ observation is highest in the African and Pacific-American sectors during September equinox. For this season, the lowest activity was reached in the Indian sector. During June solstice, peaks in $D_B$ were observed in the African, Indian and Pacific sectors, while the least was around the American-Atlantic sector. March equinox peaked around the Pacific-American sectors boundary. December solstice on the other hand, peaked around longitude $280^0$ ($-80^0$) in the American sector, while the least $D_B$ value was recorded over the Pacific sector. Generally, there is no particular trend or longitudinal asymmetry in the response of the percentage mean number of bubbles per trip containing bubbles ($D_B$). However, it is still necessary to mention that the percentage seasonal peaks in the occurrence rate of $D_B$ in descending order are September equinox, June solstice, March equinox and December solstice, with percentage values of 6.92, 5.24, 4.64, and 3.93% respectively in similar order. Table 2 presents the average percentage seasonal variation in $D_B$ for different longitudinal sectors. Unarguably, the highest percentage occurrence activity was observed for the African sector for all seasons except during December solstice (with highest sectorial percentage magnitude of 6.52 in the Atlantic sector). As a whole, the occurrence activity rate of $D_B$ was lower during the solstices when compared with the equinoxes for all sectors considered.

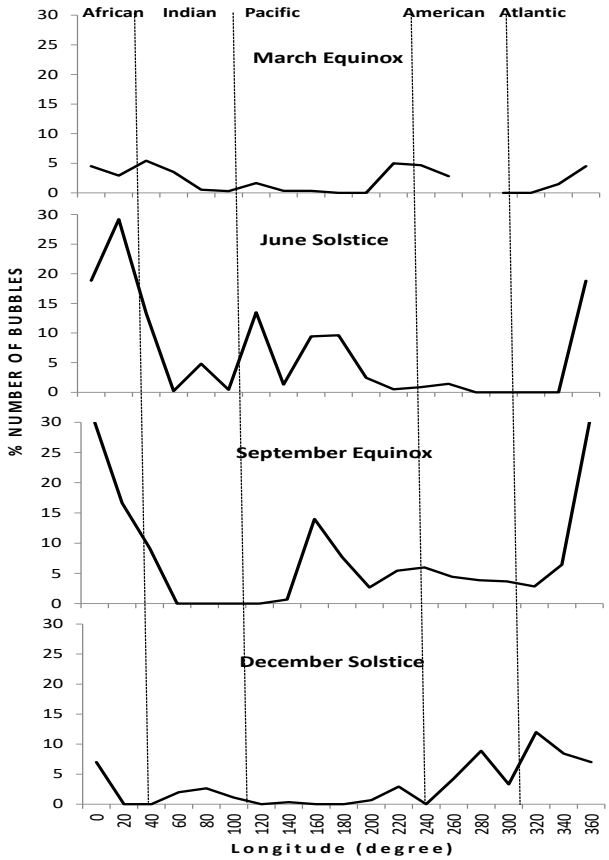


**Figure 2** Seasonal observation of percentage plasma bubble occurrence rate as a function of geographic longitude for the five sectors

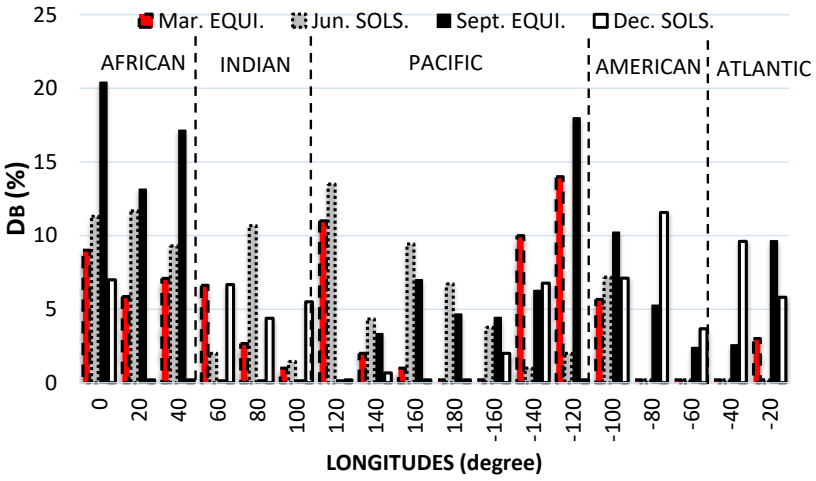


**Figure 3** Bar chart showing the seasonal and longitudinal variability of the mean number of bubbles per trip containing bubbles ($D_B$). ($D_B$ is the percentage ratio of number of bubbles ($B$) to the number of trips with bubbles ($T_B$)).

The observation in figure 4 is similar to the one in figure 3, except that it represents the plot of the percentage mean number of bubbles per trip for all trips, ($D_T$). Similar patterns were almost recorded in both figures 3 and 4 for the equinoxes, except for corresponding varying magnitudes. However, higher variations, both in magnitude and pattern were observed for the solstice seasons. However, the $D_B$ plot in figure 3 and the plasma bubble occurrence rate in figure 2 revealed that the plasma bubble occurrence is hindered in the American-Atlantic region during June solstice, with significant values in the Pacific region. Furthermore, the inhibition of the occurrence rate spreads to the Pacific region during the December solstice. These observations are consistent with the result obtained by Su et al., (2006).

**Table 2** Percentage seasonal variation in $D_B$ for different longitudinal sectors

| Season | Percentage DB | | | | |
|---|---|---|---|---|---|
| | **African** | **Indian** | **Pacific** | **American** | **Atlantic** |
| March Equinox | 7.32 | 3.43 | 4.88 | 6.56 | 3.00 |
| June Solstice | 10.76 | 4.70 | 5.28 | 2.29 | 2.83 |
| September Equinox | 16.90 | 1.27 | 5.46 | 8.97 | 8.75 |
| December Solstice | 2.33 | 5.52 | 1.87 | 5.59 | 6.52 |

Note: bolded values indicate highest percentage occurrence rates for each row of sectorial observations

## 4. DISCUSSION AND COMPARISON WITH PAST RESULTS

Makela et al (2004) had analysed data covering over 298 nights of airglow and GPS scintillation collected from January 2002 and August 2003 (a near solar maximum period) from Hawaii to obtain the pattern of the seasonal occurrence rate of equatorial plasma bubbles in the Pacific sector ($203^0$E). They recorded a broad peak of occurrence in the data from June to October to be 62%. In our result, seasonal plasma bubble data for the Pacific sector alone for both June solstice and September equinox, which spans May-October, recorded a total of 76%. These two results agree. Though our percentage observation seems to be a bit higher. Moreover, our bubble data for the entire five selected sectors recorded 73% occurrence rate for the May-October periods. Nishioka et al (2006) had investigated occurrence rate of plasma bubble using data from GPS-TEC obtained from the Japan Agency

for Marine-Earth Science and Technology across the entire longitudinal sectors, and observed that the yearly variability was highest in part, in the African sector. This also was confirmed in our study.

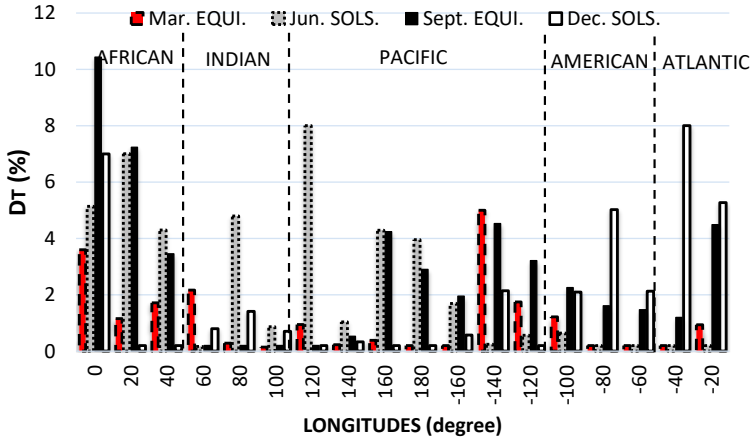


**Figure 4** Same as in figure 3, but for the mean number of bubbles per trip for all trips, ($D_T$). ($D_T$ is the $B/T_T$ ratio).

The observed greater equatorial plasma bubble occurrence rate between September equinox and December solstice in the American sector agrees with the results obtained by Tsunoda (1985) over the Brazilian sector, who proposed that plasma bubble occurrence rates should be highest when the angle between the magnetic flux tubes and the day-night terminator approaches 0°. Consequently, the E-region conductivity on either side of the flux tube is least. This is because a one side sun-lit flux tube would automatically cause an enhancement in the flux tube integrated E-region conductivity and subsequently inhibit the intensification of the Rayleigh-Taylor instability mechanism (Sultan, 1996).

Maruyama and Matuura (1984) had observed that irregularities were most rampant when the distribution of plasma density around the magnetic equator was symmetric, otherwise, the distribution was short of irregularities; and concluded that the necessary condition for the growth of equatorial plasma bubbles is the absence of a trans-equatorial thermospheric wind in the magnetic meridian. They actualize this by presenting a framework in which the trans-equatorial neutral wind acted as a hindrance to the growth of the Rayleigh-Taylor instability process. Kim et al. (2002), had used data spanning April 1965-October 1968 from azimuth-scanning photometric observations from the Haleakala Volcano during a period of minimum and increasing solar activity, to observe a maximum plasma bubble occurrence rate in September-October, with an additional maximum, slightly lower in magnitude, in April. This observation is similar to the one observed in the present study during September equinox (except over Indian sector) and June solstice respectively.

In another work closely related to the years used in this work, McClure et al. (1998) investigated the occurrence rate of equatorial ionospheric anomalies based on data collected from the ion drift meter on the AE-E satellite from January 1978-September 1980 over the Pacific region. They recorded percentage occurrence rates of 30, 25, 15 and 8% respectively for the May-June-July, August-September-October, February-March-April and November-December- January periods. In the present study, we recorded 40, 38, 14 and 8% respectively in similar order for the Pacific sector observation. The two results are similar in that (i) same seasonal trend was observed with highest percentage of occurrence during June solstice, and the least in December solstice (ii) the difference in the percentage occurrence rate during June solstice (10%) and September equinox (13%) between the two results may have been due to

the inclusion of extra database (i.e. January-September 1980) into the work of McClure et al. (1998).

One striking event that was observed in the present study, but not mentioned by earlier works cited is that seasons with the highest occurrence rate of plasma bubbles (i.e. from figure 2) are characterized with corresponding higher correlation coefficients of total number of trips ($T_T$)/trips with bubbles ($T_B$) relation. This is indicated in figure 5, where June solstice and September equinox recorded $T_T/T_B$ correlation values of $R$ = 0.8270 and 0.7543 respectively. Observe that $R$ value is low for both March equinox (0.2324) and December solstice (0.0447), just as they both recorded lower percentage occurrence rates of plasma bubble. Recall from section 2 that March equinox and December equinox recorded 10 and 16% respectively, while 34 and 39% occurrence rates were recorded for June solstice and September equinox respectively.

Similar feat was observed for the $T_T/T_B$ correlation relation for the longitudinal sectors in figure 6. Here, higher correlation values were recorded for the African ($R$ = 0.8006), Atlantic (0.7001), and Pacific (0.6107) sectors. These three sectors recorded the highest occurrence rate of plasma bubble manifestation, as indicated earlier in figure 2. Further, both the American and Indian sectors that recorded lower activity rates of plasma bubble had $R$ values of 0.100 and 0.2739 respectively for the $T_T/T_B$ correlation relation. It can therefore be suggested that the $R$ value for $T_T/T_B$ correlation relation is an indicator of the occurrence rate magnitude both seasonally and longitudinally. Li et al (2008) had proposed that the small-scale longitudinal variation of plasma bubble occurrence rates may have originated from the evening equatorial ionization anomaly small-scale longitudinal structures, and concluded that the evening pre-reversal E x B drifts, together with the longitudinal variations of evening EIA, are assumed to play a role in determining the longitudinal variations of equatorial and low-latitude plasma bubble occurrence rates. The EIA is believed to be generated by the fountain effect, which consists of plasma enhancement at the magnetic equator by eastward electric fields (Adebesin et al 2013a, 2013b) and consequent redistribution along the magnetic field lines to higher latitudes.

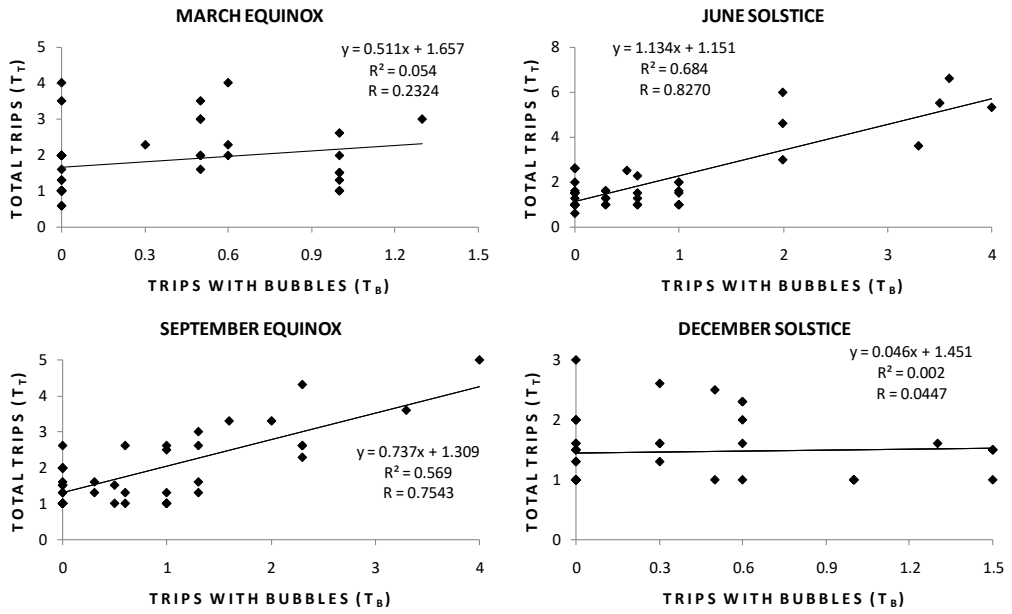


**Figure 5** Correlation plot of total number of trips ($T_T$) with number of trips with bubbles ($T_B$) for each season.

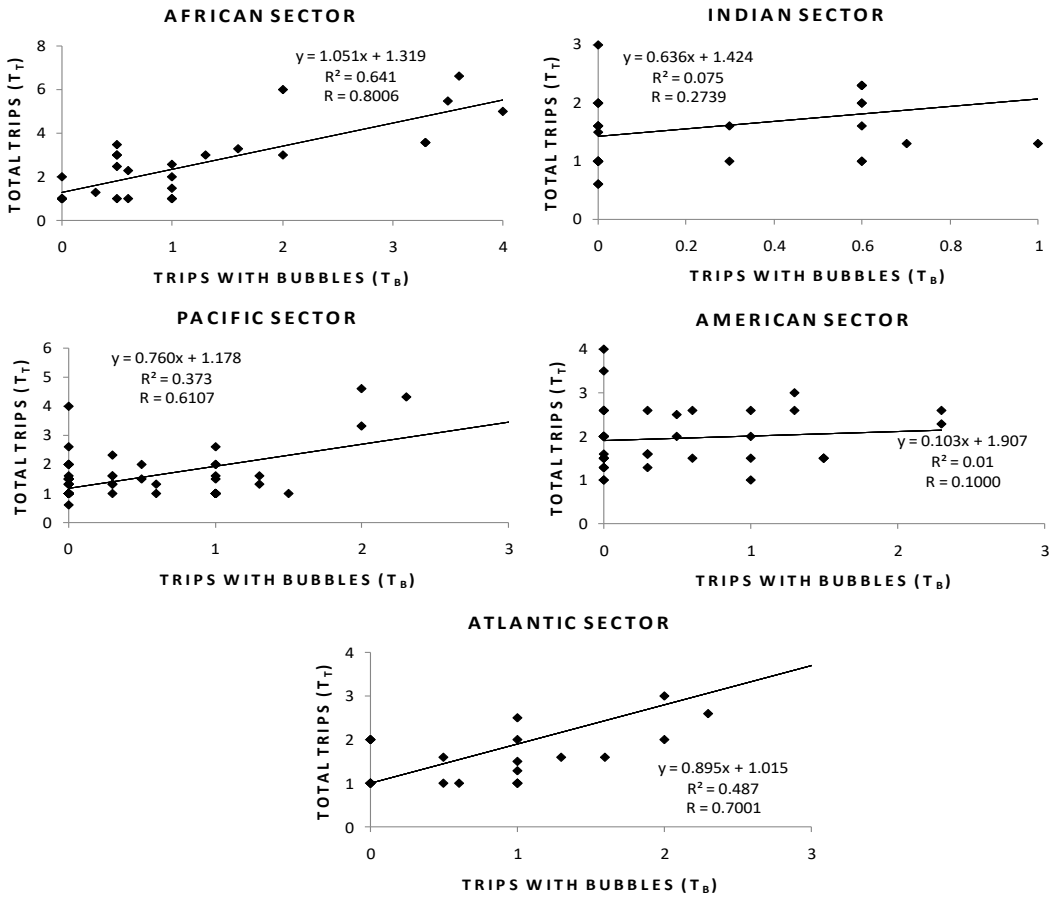


**Figure 6** Correlation plot of total number of trips ($T_T$) with number of trips with bubbles ($T_B$) for each sector.

## 5. SUMMARY AND CONCLUSION

A striking result in the present study is that different longitude sectors have different plasma bubble seasons/activities. In order to evaluate the longitudinal and seasonal effects on plasma bubble occurrence, orbits were divided into five longitude sectors. These include the African, Indian, Pacific, American and Atlantic sectors. The highest occurrence rate of plasma bubble was in the African-Atlantic sector for all seasons. However, the lowest occurrence rates over different sectors were seen to differ from one season to another, and are attributed to different magnetic declination angle, and also to the conductivity gradient in the F-region. Seasonally, the highest bubble occurrence rate was in September equinox (39%). The occurrence activity rate of $D_B$ defined as the percentage ratio of number of bubbles ($B$) to the number of trips with bubbles ($T_B$) was higher during the equinoxes than at solstices for all longitudinal sectors.

Generally, no particular pattern was observed in the response of the percentage mean number of bubbles per trip containing bubbles ($D_B$) both seasonally and longitudinally, it is still necessary to mention that the peaks during the equinoxes, as observed around the Pacific-American sector boundary suggests that the active growth region during these periods is to the west of the globe. Further, higher occurrence rate of plasma bubbles is characterized by corresponding higher correlation coefficients of total number of trips ($T_T$) to trips with bubbles ($T_B$) relation. Similarly, higher $T_T/T_B$ correlation values were recorded for the sectors with higher occurrence rate of plasma bubble manifestation, and vice-versa. We therefore

suggest that the $R$ value for $T_T/T_B$ correlation relation is an indicator to the occurrence rate magnitude both seasonally and longitudinally. The results of some past works were validated in this study.

## REFERENCES


[1] Abdu, M. A. (2001): Outstanding problems in the equatorial ionosphere thermosphere electrodynamics relevant to spread F, J. Atmos. Solar-Terr. Phys., 63, 869–884.

[2] Adebesin B.O., A. B. Rabiu, O. K. Obrou, and J. O. Adeniyi (2018a): Ionospheric peak electron density and Performance evaluation of IRI-CCIR near magnetic equator in Africa during two extreme solar activities. Space Weather, 16(3), 230-244, doi: 10.1002/2017SW001729

[3] Adebesin B.O., Adeniyi J.O., Oladipo O.A, Olawepo A.O., and Adimula I.A. (2018b): Quantitative Characteristics of Equatorial Ionization Gradient above 150km at Low Solar Activity. Radio Science. 53, doi:10.1029/2018RS006560. In press.

[4] Adebesin B.O., A. B. Rabiu, O. S. Bolaji, J. O. Adeniyi, and C. Amory-Mazaudier (2018c): Ionospheric Climatology at Africa EIA trough stations during Descending Phase of Sunspot Cycle 22. Journal of Atmospheric and Solar-Terrestrial Physics. 172, 83-99, doi:10.1016/j.jastp.2018.03.00.

[5] Adebesin, B. O. Pulkinnen Antti, Ngwira Chigomezya (2016): The Interplanetary and Magnetospheric Causes of Extreme dB/dt at Equatorial Locations. Geophysical Research Letters. 43 (22), 11,501-11,509. doi:10.1002/2016GL071526

[6] Adebesin B.O, Adeniyi J.O., Adimula I.A, Oladipo O.A, Olawepo A.O and Reinisch B.W. (2015a): Comparative Analysis of Nocturnal Vertical Plasma Drift velocities inferred from Ground-based ionosonde measurements of hmF2 and h'F. Journal of Atmospheric and Solar Terrestrial Physics. 122, 97-107. doi: 10.1016/j.jastp.201 4.11.

[7] Adebesin, B. O., A. B. Rabiu, J. O. Adeniyi, C. Amory-Mazaudier (2015b): Nighttime morphology of vertical plasma drifts at Ouagadougou during different seasons and phases of sunspot cycles 20-22. Journal of Geophysical Research – Space Physics, 120(11), 10,020-10,038. doi:10.1002/2015JA021737

[8] Adebesin B. O, Adekoya B. J., Ikubanni S. O., Adebiyi S. J., Adebesin O. A., Joshua B. W., and Olonade K. O. (2014): Ionospheric foF2 morphology and response of F2 layer height over Jicamarca during different solar epochs and comparison with IRI-2012 model. .Journal of Earth System Science. 123(4), 751-765. doi:10.1007/s12040-014-0435-y.

[9] Adebesin B.O., Adeniyi J.O., Adimula, I.A., and Reinisch, B.W. (2013a): Low latitude Nighttime Ionospheric vertical E x B drifts at African Region. Advances in Space Research. 52(12), 2226-2237. doi: 10.1016/j.asr.2013.09.033.

[10] Adebesin B.O., Adeniyi, J.O., Adimula, I.A., Reinisch, B.W., and K. Yumoto. (2013b): F2 layer characteristics and electrojet strength over an Equatorial station. Advances in Space Research. 52(5), 791-800. doi:10.1016/j.asr.2013.05.025.

[11] Adebesin B.O, Adeniyi J.O., Adimula I.A and Reinisch B.W (2013c): Equatorial vertical plasma drift velocities and electron densities inferred from ground-based ionosonde measurements during low solar activity: Journal of Atmospheric and Solar Terrestrial Physics, 97, 58-64, http://dx.doi.org/10.1016/j.jastp.2013 .02.010,2013.

[12] Adebiyi, S.J., Odeyemi, O.O., Adimula, I.A., Oladipo, O.A., Ikubanni, S.O., Adebesin B.O., and Joshua, B.W. (2014a): GPS derived TEC and foF2 variability over an equatorial station and the performance of IRI-model. Advances in Space Research. 54, Issue 4, 565-575. doi:10.1016/j.asr.2014.03.026.

[13] Adebiyi, S.J., Adimula, I.A., Oladipo, O.A., Joshua, B.W., ADEBESIN B.O., and Ikubanni, S.O. (2014b): Ionospheric Response to a Magnetic Activity at Low and Mid-latitude stations. Acta Geophysica, 62(4), 973-989. DOI: 10.2478/s11600-014-0205-x.

[14] Adeniyi J.O., Adebesin B.O, Adimula I. A, Oladipo O.A, Olawepo A.O Ikubanni, S.O and Reinisch B.W. (2014): Comparison between African Equatorial Station Ground-based inferred vertical E x B drift, Jicamarca direct measured drift, and IRI model. Advances in Space Research, 54, Issue 7, 1629-1641. doi:10.1016/j.asr.2014.06.0 14

[15] Aarons, J. (1993): The longitudinal morphology of equatorial F layer irregularities relevant to their occurrence, Space Sci. Rev., 63, 209.

[16] Basu, B. (1997): Generalized Rayleigh-Taylor instability in the presence of time-dependent equilibrium, J. Geophys. Res., 102, 17 305.

[17] Burke W. J, C. Y. Huang, L. C. Gentile, and L. Bauer (2004): Seasonal-longitudinal variability of equatorial plasma bubbles, Annales Geophysicae, 22: 3089–3098, SRef-ID: 1432-0576/ag/2004-22-3089

[18] Burke, W. J., Maynard, N. C., Hagan, M. P., Wolf, R. A., Wilson, G. R., Gentile, L. C., Gussenhoven, M. S., Huang, C. Y., Garner, T. W., and Rich, F. J. (1998): Electrodynamics of the inner magnetosphere observed in the dusk sector by CRRES and DMSP during the magnetic storm of June 4–6, 1991, J. Geophys. Res., 103, 29 399.

[19] Eccles, J. V. (1998): A simple model of low-latitude electric fields, J. Geophys. Res., 103, 26 699.

[20] Gentile, L.C., Burke, W.J., Rich, F.J., (2006). A global climatology for equatorial plasma bubbles in the topside ionosphere. Annales Geophysicae. 24,163.

[21] Huang, C. Y., Burke, W. J., Machuzak, J. S., Gentile, L. C., and Sultan, P. J. (2001): DMSP observations of equatorial plasma bubbles in the topside ionosphere near solar maximum, J. Geophys. Res., 106, 8131.

[22] Kim, Y. H., Hong, S. S., and Weinberg, J. L. (2002): Equatorial spread F found in 5577 °A and 6300 °A airglow observations from Hawaii, J. Geophys. Res., 107, 1264, doi: 10.1029/2001JA009 232.

[23] Lee C.C., J. Y. Liu, B. W. Reinisch, W.S. Chen, and F.D. Chu. (2005): The effects of the pre-reversal drift, the EIA

[24] asymmetry, and magnetic activity on the equatorial spread F during solar maximum, Annales Geophysicae, 23, 745–751.

[25] Li, G., B. Ning, L. Liu, B. Zhao, X. Yue, S.-Y. Su, and S. Venkatraman (2008), Correlative study of plasma bubbles,

[26] evening equatorial ionization anomaly and equatorial pre-reversal E x B drifts at solar maximum, Radio Sci., 43, RS4005, doi: 10.1029/2007RS003760.

[27] Magdaleno S, M.Cueto, M. Herraiz, G.Rodrıguez-Caderot, E. Sardo, I. Rodrıguez (2013): Ionospheric bubbles detection algorithms: Analysis in low latitudes, Journal of Atmospheric and Solar-Terrestrial Physics 95–96, 65–77.

[28] Makela J. J, B. M. Ledvina, M. C. Kelley, and P. M. Kintner (2004): Analysis of the seasonal variations of equatorial plasma bubble occurrence observed from Haleakala, Hawaii, Annales Geophysicae, 22, 3109–3121, SRef-ID: 1432-0576/ag/2004-22-3109

[29] Maruyama, T. and N. Matuura (1984), Longitudinal variability of annual changes in activity of equatorial spread F and plasma bubbles, Journal of Geophysical Research, 89, 10903-10912.

[30] McClure, J. P., Singh, S., Bamgboye, D. K., Johnson, F. S., and Kil, H. (1998): Occurrence of equatorial F region irregularities: Evidence for tropospheric seeding, J. Geophys. Res., 103, 29 119–29 135.

[31] Nishioka, M, Saito A, Fukao, S, Yamamoto M, Otsuka, Y.; Tsugawa T. (2006): Occurrence characteristics of plasma bubble derived from global GPS-TEC data American Geophysical Union, Fall meeting 2006, 2006AGUFMSA33B0284N

[32] Oyekola, O. S. (2009): A study of evolution/suppression parameters of equatorial post-sunset plasma instability. Ann. Geophys. 27, 1–5.

[33] Sahai, Y, J. Aarons, M. Mendillo, J. Baumgardner, J. A. Bittencourt, and H. Takahashi. (1994): 01630 nm imaging observations of equatorial plasma depletions at 160 S dip latitude, Journal of Atmospheric and Terrestrial Physics, 56 (11), 1461-1475.

[34] Su, S.-Y., C. H. Lin, H. H. Ho, and C. K. Chao (2006), Distribution characteristics of topside ionospheric density irregularities: Equatorial versus mid-latitude regions, J. Geophys. Res., 111, A06305, doi:10.1029/2005 JA0113 30.

[35] Sultan, P. J. (1996): Linear theory and modelling of the Rayleigh-Taylor instability leading to the occurrence of equatorial spread F, Journal of Geophysical Research, 101, 26875-26891.

[36] Terra, P. M., J. H. A. Sobral, M. A. Abdu, J. R. Souza, and H. Takahashi (2004): Plasma bubble zonal velocity

[37] variations with solar activity in the Brazilian region, Annales Geophysicae, 22: 3123–3128.

[38] Tsunoda, R. T. (1985): Control of the seasonal and longitudinal occurrence of equatorial scintillations by the longitudinal gradient in integrated E region Pedersen conductivity, Journal of Geophysical Research, 90, 447-456.

[39] Woodman, R. F. and LaHoz, C. (1976): Radar observations of F region equatorial irregularities, J. Geophys. Res., 81, 5447.